Self-Organized Lipid-Porphyrin Bilayer Membranes in Vesicular Form: Nanostructure, Photophysical Properties, and Dioxygen Coordination

Teruyuki Komatsu, Miho Moritake, Akito Nakagawa, and Eishun Tsuchida*[a]

Abstract: An amphiphilic tetraphenylporphyrin and its iron complex bearing four phospholipid substituents, in which a trimethylolethane residue connects the two acyl chains (lipid-porphyrins), have been synthesized. The free-base lipid-porphyrin **6a** self-organizes in aqueous media to form spherical unilamellar vesicles with a diameter of 100 nm and a uniform thickness of 10 nm, which corresponds to twice the length of the molecule. In the visible absorption spectrum, the porphyrin Soret band was significantly red-shifted (12 nm) relative to that of the monomer in benzene/MeOH solution due to the excitonic interaction of the porphyrin chromophores. The $\Pi - A$ isotherm of **6a** gave an area per molecule of 2.2 nm^2, which allowed the estimation of the number of molecules in a single vesicle (2.3×10^4). Double-layered Langmuir–Blodgett (LB) films of **6a** on a glass surface exhibited an absorption spectrum identical to that of the **6a** vesicles in bulk aqueous solution, and this suggests that they contain similar geometric arrangements of the porphyrin moieties. Exciton calculations on the basis of our structural model reproduced the bathochromic shift of the Soret band well. In the photophysical properties of the **6a** vesicles, the characteristics of J-aggregated porphyrins substantially predominate: strong fluorescence and extremely short triplet lifetime. The iron complex **6b** with a small molar excess of 1-dodecylimidazole (DIm) also formed spherical unilamellar vesicles (100 nm Φ). Scanning force microscopy after evaporation on a graphite surface revealed **6b**/DIm vesicles with a vertical height of 19.8 nm, which coincided with the thickness of the double bilayer membranes. The ferrous **6c** formed a bis(DIm)-coordinated low-spin Fe^{II} complex under an N_2 atmosphere. Upon addition of O_2 to this solution, a kinetically stable O_2 adduct was formed at 37 °C with a half-life of 17 h. Distinct gel-phase (liquid-crystal) transitions of the lipid-porphyrin membranes were clearly observed; the free base **6a** displayed a higher transition temperature (56 °C) than the iron complex. Magnetic circular dichroism and infrared spectroscopic studies proved that molecular O_2 coordinates to the self-organized lipid-porphyrinatoiron(II) vesicles in aqueous media.

Keywords: dioxygen ligands · nanostructures · porphyrinoids · self-assembly · vesicles

Introduction

It is of current interest to construct self-organized porphyrin assemblies by formation of noncovalent bonds (metal–ligand coordination, hydrogen bonding, and electrostatic attraction) to mimic the diverse biological reactivity of porphyrinoids in nature.[1, 2] Such vectorial binding forces have built highly complicated porphyrin architectures that are difficult to prepare by general organic synthetic procedures. However, most of them were prepared in organic solvents. If we are to reproduce the various biochemical reactions that rely on the natural porphyrins, aqueous systems are particularly important. Hence, over the past few decades substantial efforts have directed towards embedding synthetic model porphyrins in phospholipid vesicles;[3] ground-state or photoinduced electron transfer,[4, 5] dioxygen (O_2) transport,[6] selective oxidation reactions,[7] and ATP production [8] have been reported. Unfortunately, the locations of the porphyrin co-factors in these ensembles are not always accurate, because of the low guest-to-host molecular ratio. To counter this problem, porphyrin amphiphiles become attractive building blocks for constructing well-defined three-dimensional porphyrin assemblies in aqueous media. Coulombic forces were first successfully employed in the preparation of beautiful porphyrin fibers, but they are relatively unstable and tend to precipitate because of their low solubility.[9] We are now convinced that hydrophobic interaction is the most useful driving force for preparing large-scale supramolecular systems in which thousands of metalloporphyrins are aligned with great regularity and longevity. Indeed, some porphyrins with amphiphilic side chains at the periphery self-organize in water to form supramolecular aggregates (fibers, tubes, vesicles, and sheets).[10, 11] A tetraphenylporphyrin (TPP) derivative with four dialkylglycerophosphocholine groups on one side of the ring plane produced spherical unilamellar

[a] Prof. E. Tsuchida, Dr. T. Komatsu, M. Moritake, A. Nakagawa
Advanced Research Institute for Science and Engineering
Waseda University, Tokyo 169-8555 (Japan)
Fax: (+81) 3-3205-4740
E-mail: eishun@waseda.jp

  0947-6539/02/0823-5469 $ 20.00+.50/0

vesicles with reversible O_2-binding ability, similar to those of hemoglobin and myoglobin under physiological conditions (pH 7.3, 37 °C).[12] The only drawback of this compound is laborious introduction of the phospholipid substituents, in which a glycerol residue connects the two acyl chains. We recently found that the role of glycerol can be adopted by a similar triol, namely, trimethylolethane. To the best of our knowledge, there has been no report on a phospholipid amphiphile involving a trimethylolethane residue as the connecting moiety of the acyl chains, and its self-assembly behavior. Here we report the first synthesis of and bilayer membrane formation by novel TPP derivatives with four phospholipid substituents on the porphyrin ring (lipid-porphyrins): free base **6a**, Fe^{III} complex **6b**, and Fe^{II} complex **6c**. The nanostructure of the lipid-porphyrin aggregate was elucidated by transmission electron microscopy (TEM) and scanning force microscopy (SFM). Exciton calculations on the basis of our bilayer model reproduces well the bathochromic shift observed in the UV/Vis absorption of the **6a** membranes. The free-base lipid-porphyrin vesicles fluoresce strongly, and the vesicles of the Fe^{II} complex formed a stable and reversible O_2 adduct under physiological conditions, with an O_2-binding affinity similar to that of human erythrocytes. Magnetic circular dichroism (MCD) and infrared (IR) spectroscopic studies on the O_2 coordination mode have also been made.

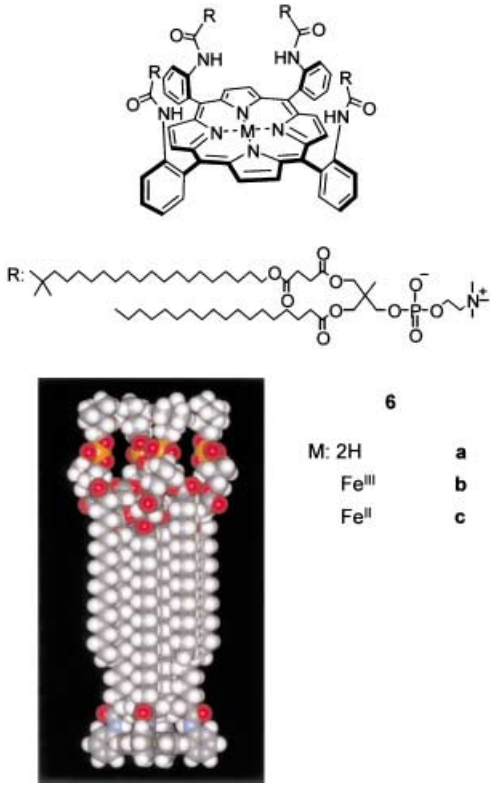

Results and Discussion

Synthesis: The synthesis of lipid-porphyrins is summarized in Scheme 1. The phospholipid precursor **3** is easily synthesized in three steps starting from trimethylolethane, whereas five

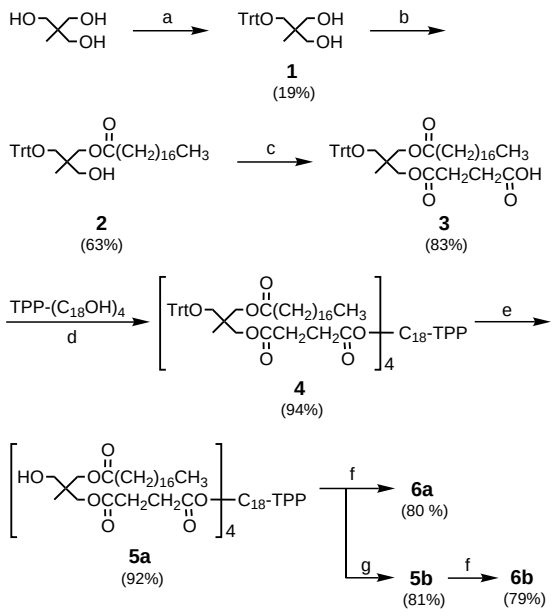

TPP-$(C_{18}OH)_4$: 5,10,15,20-Tetrakis{α,α,α,α-*o*-(2,2-dimethyl-20-hydroxyicosanamido)phenyl}porphine

Scheme 1. Synthetic scheme for lipid-porphyrin **6a** and its iron(III) bromide complex **6c**. a) Trityl chloride/DMF, pyridine. b) Stearic acid anhydride, 4-DMAP/THF. c) Succinic acid anhydride/THF. d) DCC, 4-DMAP/CH_2Cl_2. e) $BF_3 \cdot Et_2O/CH_2Cl_2$. f) 2-chloro-1,3,2-dioxaphospholane 2-oxide/CH_2Cl_2, TEA. g) $FeBr_2$/THF, 2,6-lutidine. DCC = dicyclohexyl carbodiimide, 4-DMAP = 4-dimethylamino pyridine.

steps are required to obtain the corresponding material from glycerol. The coupling of **3** with the parent TPP derivative TPP-$(C_{18}OH)_4$[13] was performed by dicyclohexyl carbodiimide (DCC) in DMF at room temperature to give **4a** in 94% yield. $BF_3 \cdot MeOH$ selectively cleaved the trityl protecting groups to yield **5a** (92%). The phosphocholine head groups were introduced in the final step by a general procedure with 2-chloro-1,3,2-dioxaphospholane 2-oxide. This is in contrast to our glycerol-based lipid-porphyrin, for which only mild, acidic phosphorylation could be used to introduce phosphocholine residues into the 3-hydroxyl group of glycerol.[12] As a result, the free-base lipid-porphyrin **6a** was synthesized in six steps by using the parent TPP-$(C_{18}OH)_4$, whereas the glycerol analogue requires twelve steps, including zinc insertion at the porphyrin center and complicated reactions in low yields. The Fe^{III} complex **6b** was prepared from **5b** in the same manner as for **6a** from **5a**; all the compounds are available in gram quantities. The α^4 structure of the porphyrins did not atropisomerize throughout the entire process, as was confirmed by ^1H NMR spectroscopy: the chemical shift of the singlet for the 2,2-dimethyl groups ($\delta = -0.4$) remained constant. For the Fe^{III} complex **6b**, ^1H NMR spectra were recorded after removing the iron center with $FeCl_2$ in HCl/acetic acid.[14] The Satisfactory analytical data were obtained for all compounds described here (see Experimental Section).

Morphology and nanostructure of the free-base lipid-porphyrin assembly: The free-base lipid-porphyrin **6a** was dispersed in deionized water by ultrasonication ([**6a**] = 1 –

0947-6539/02/0823-5470 $ 20.00+.50/0 *Chem. Eur. J.* **2002**, *8*, No. 23

3000 μM) to give a red solution that was stable for a year without precipitation. The TEM of the negatively stained and evaporated sample revealed that **6a** forms perfectly spherical vesicles with a diameter of 100 nm (Figure 1a). The thickness

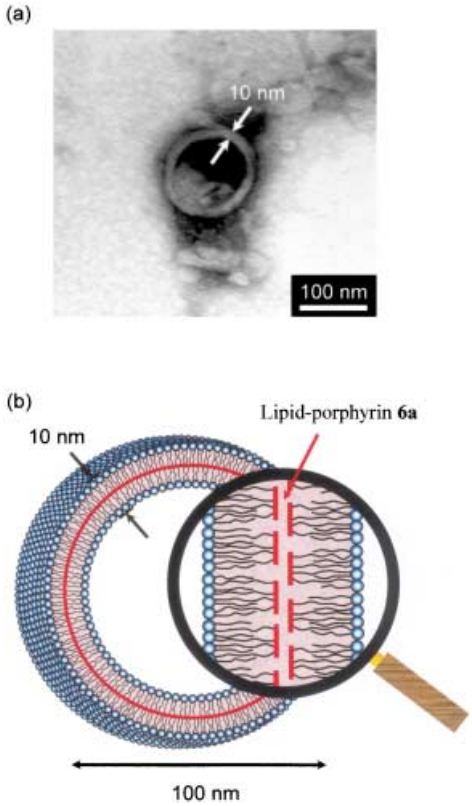

Figure 1. a) Transmission electron micrograph of a vesicle of the free-base lipid-porphyrin **6a** negatively stained with uranyl acetate. b) Schematic of the bilayer membrane.

of the unilamellar membrane was 10 nm, which corresponds to twice the length of the **6a** molecule (4.6 nm) (Figure 1b). Light-scattering measurements gave a sharp peak with a narrow distribution (100 ± 36 nm) and supported the TEM result. In general, ultrasonic irradiation of phospholipids provides small unilamellar vesicles. However, the spherical membrane consisting of the giant porphyrin amphiphile **6a** ($M = 4564$) cannot produce a large curvature; therefore, the vesicles are much larger than the usual ones. They neither coagulate nor photodegrade for a long time.

The visible absorption spectrum of the **6a** vesicles showed a porphyrin Soret band at 434 nm ($\varepsilon_{max} = 3.1 \times 10^5\,M^{-1}cm^{-1}$), which was significantly shifted to the red region relative to that of the monomer in benzene/MeOH (4:1; $\lambda_{max} = 422$ nm; Figure 2). The bandwidth at half-height ($\Delta\lambda_{1/2} = 16$ nm) was slightly wider than that of the monomer ($\Delta\lambda_{1/2} = 14$ nm). The intensity and absorption maxima of the Q-bands demonstrated even smaller shifts of 3 nm, which may be a van der Waals shift caused by the replacement of solvent. Thus, the larger bathochromic shift of the Soret band (12 nm) should include some excitonic interactions owing to a lateral arrangement (J-aggregate) of the transition moments of the porphyrin

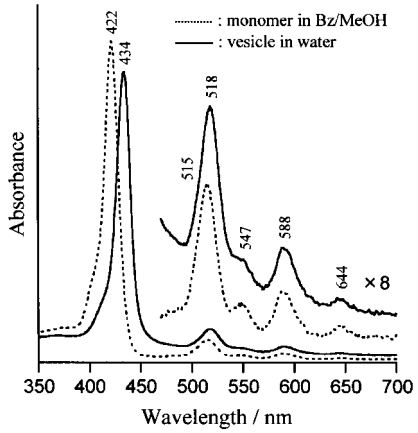

Figure 2. UV/Vis absorption spectra of lipid-porphyrin **6a** at 25 °C.

chromophores. Hence, we are certain that the hydrophobic TPP planes of **6a** form two-dimensional planar sheets in the vesicles, and stack at the middle of the bilayer membranes (Figure 1b). The quantitative evaluation of the excitonic interactions of these stacked porphyrin sheets are described below.

Surface pressure–molecular area ($\Pi - A$) isotherm and exciton calculation of the Langmuir-Blodgett (LB) film: The $\Pi - A$ isotherm of the giant porphyrin amphiphile **6a** exhibited essentially the same features as that of typical amphiphilic lipids (Figure 3).[15] At large areas

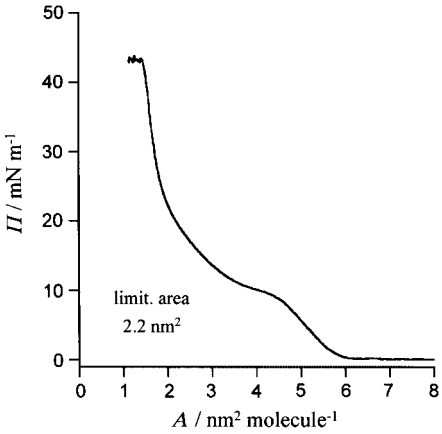

Figure 3. $\Pi - A$ isotherm of lipid-porphyrin **6a**. The subphase was pure water, and the film was compressed at a rate of 10 mN min^{-1}.

(> 6.0 nm^2 molecule^{-1}) the film is in an expanded state. Upon compression, the film undergoes a transition from the expanded phase to the liquid expanded phase (4.5 nm^2 molecule^{-1}). Further compression led to the liquid-expanded/liquid-condensed transition (3.5 nm^2 molecule^{-1}), and finally to a solid condensed phase. The collapse pressure reached 43 mN m^{-1}, and this indicates formation of a relatively close packed solid membrane. Extrapolation of the second linear portion of the isotherm to zero surface pressure gave, as the intercept, the area per **6a** molecule. The value of 2.2 nm^2 coincides with the sum of the areas of four phosphocholine head groups, and we infer that the lipid-porphyrin in

  0947-6539/02/0823-5471 $ 20.00+.50/0

the oriented layer is likely to have a cylindrical form with a TPP bottom of 1.5 nm^2 (see the space-filling model above). Based on this value, the number of constituent molecules of **6a** in one vesicle (100 nm Φ) was estimated to be 2.3×10^4 (1.4×10^4 in the outer phase and 9.0×10^3 in the inner phase).

The **6a** monolayer on the LB trough was then slowly transferred onto a glass plate to give a porphyrin monolayer in which the hydrophilic head groups likely face the glass surface, while the hydrophobic TPP plane is toward the air. Further immersion and removal of the substrate perpendicular to the trough should result in formation of trilayered LB films. Interestingly, the visible absorption spectra of these films provided good clues to the in-plane and interlayer arrangements of the TPP moieties in the **6a** vesicles. The monolayer showed distinct TPP absorption with sufficiently high intensity for spectroscopic analysis (Figure 4a). The Soret band at 430 nm is clearly red-shifted (8 nm) relative to that of the monomer in benzene/MeOH ($\lambda_{max} = 422$ nm). The absorption intensity of the **6a** trilayers is three times as high as that of the monolayer with a small bathochromic shift (2 nm) in the Soret band; the λ_{max} of the Q-bands were essentially unaltered. This observation suggested formation of triple-layer **6a** films on the glass plate. Here, it is of interest to subtract the spectrum of the monolayer from that of the trilayer, presumably to give the absorption of a bilayer in which the outer and inner TPP sheets are stacked at the center of the membrane (Figure 4b). In fact, the difference spectrum ($\lambda_{max} = 433$, $\Delta\lambda_{1/2} = 15$ nm) closely resembles that of the **6a** vesicles in bulk aqueous solution ($\lambda_{max} = 434$, $\Delta\lambda_{1/2} = 16$ nm, Figure 2), that is, the spherical **6a** vesicles and double-layered films on a solid substrate contain similar porphyrin arrangements.

Then we employed simple point-dipole exciton coupling theory to predict the porphyrin alignment in the LB mono- and bilayers.[16] First, for the **6a** monolayer film on the glass surface, we assumed that the tightest packing of the TPP moieties is realized by a rhomboidal lattice with diagonal distances of 2.6 nm for $2a$ and 1.48 nm for $2b$ (Figure 4c), as observed in the triclinic unit cell of a single crystal of unsolvated free-base TPP.[17] The head-group area of 2.2 nm^2 could be fitted on an individual porphyrin platform without overlap. This assumption was also made in our excitonic calculation on the monomolecular porphyrin platelets.[11h] The exciton interaction ΔE between two porphyrins is given by Equation (1):

$$\Delta E = M^2 r_{mn}^{-3}(1 - 3\cos^2\theta) \quad (1)$$

where M is the transition dipole moment of **6a**, r_{mn} is the center-to-center distance between the original porphyrin (P_o) and neighboring porphyrin (P_{mn}), and θ is the tilt angle between the line connecting the centers and the molecular axes. We took into account all the interactions with the infinite porphyrin neighbors on the 22 lines through the origin of the coordinate axes. The excitonic interaction ΔE is always considered as V_{mn} and V'_{mn} in two different Soret transitions S_x and S_y (see Experimental Section). With our **6a** monolayer model, the difference was very small. With $M^2 = 81.8\,D^2$ for the dipole strength of the monomer, total V and V' were calculated to be -519.9 and -515.4 cm^{-1}, respectively. The wavelength difference between the corresponding transitions is much smaller than the half-width of the Soret band of the monomer. Consequently, splitting of the Soret band could not

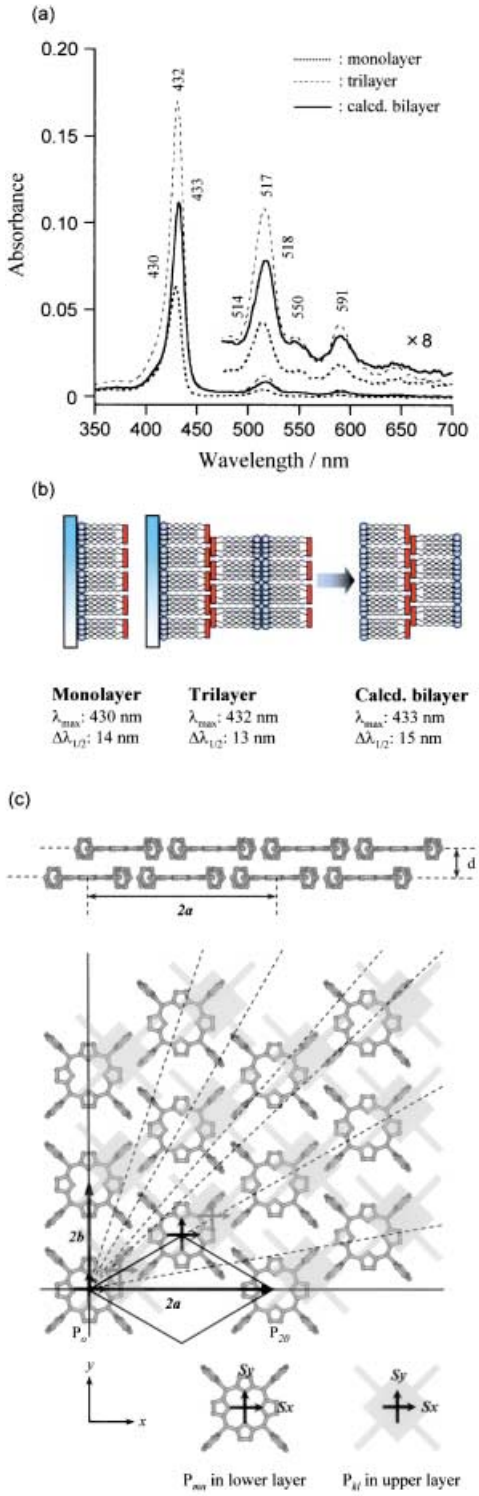

Figure 4. a) UV/Vis absorption spectra of LB films of lipid-porphyrin **6a** on a glass plate at 25 °C. b) Schematics of the mono-, tri-, and bilayers of lipid-porphyrin **6a** on the glass surface. c) Predicted arrangement of the porphyrin planes as a model for the bilayer membranes of lipid-porphyrin **6a**. The porphyrin P_o is located at the origin of the coordinate axes.

0947-6539/02/0823-5472 $ 20.00+.50/0 *Chem. Eur. J.* **2002**, *8*, No. 23

be expected, and the result was one exciton band, red-shifted by 517.7 cm^{-1} with respect to the monomer. This calculated shift is almost identical to the observed value of the **6a** monolayer (only 76.8 cm^{-1} larger). A van der Waals shift, which occurs on going from solution to a dense-packed LB film, was not seen. The real lattice of the LB monolayer might be slightly different from our model, because of the direct contact between the phosphocholine head groups and the solid glass surface. The use of an extended transition dipole instead of the point dipole also gave nearly the same results.[18, 19]

To predict the absorption of the bilayer, we made the additional hypothesis that the interlayer TPP arrangements are also similar to those found in crystals of free-base TPP. Based on the structural data reported by Strauce et al., two postulates are made: 1) a slipped face-to-face stacking of the porphyrin sheets with a minimum spacing d of 4.1 Å (Figure 4c),[17] and 2) a porphyrin core in the upper layer is shifted by +4.0, +2.7, and +4.1 Å in the x, y, and z directions, respectively, from the center of the nearest core in the layer below. The distances and angles from the porphyrin P_o to the neighbors in the upper layer were estimated. Then we calculated all the interactions of these porphyrin pairs (total of 46 combinations), but stopped summation at a distance of some 5 nm. The difference was relatively wide in this calculation: −805.9 and 323.8 cm^{-1} for S_x and S_y, respectively. If this is true, the Soret bands should be split or blue-shifted with significant broadening. However, the reverse was the case; only a 3 nm bathocromic shift from the monolayer and still narrow bandwidth were observed. In our structural model, the most unreliable parameter is the layer spacing d. For a slightly larger value of $d = 6.0$ Å the difference decreased (−152.0 and 268.2 cm^{-1} for the x and y directions). This means a rather small shift from λ_{max} of the monolayer, and is in good agreement with the fact that the absorptions of the monolayer and the bilayer are quite similar (Figure 4a). Since the spherical **6a** vesicles in bulk aqueous solution showed a spectrum similar to that of the double-layered LB films of **6a** on the glass plate, we can conclude that they are both describable by equivalent exciton interactions. The small wavelength difference between the predicted λ_{max} in our model (431 nm) and experimentally obtained values (λ_{max} = 433 nm on the glass surface and 434 nm in water) is likely due to the van der Waals shift. In this case, the head group–glass contact effect, which was considered in the monolayer, can be ignored, since the stacking of the second porphyrin layer probably weakens it. Of course, the porphyrin lattice in the bilayers is somewhat flexible, because of the fluidity of the membrane, despite its being below the phase transition temperature (vide infra); therefore, the observed shift in the Soret band always comes from the averaged exciton interaction.

Photophysical properties of free-base lipid-porphyrin vesicles: The most remarkable photophysical property of the aqueous solution of **6a** vesicles is to fluoresce strongly; its fluorescence emission intensity was 76% of that of the monomer in benzene/MeOH (4:1; Figure 5). The three-dimensional excitation–emission spectrum revealed that the fluorescence emission maxima (λ_{em} = 649, 713 nm) correlates with the Soret band absorption of the vesicles (λ_{max} = 434 nm), which indicates that the strong fluorescence is due to the membrane, and not to a small amount of monomer dissociated from the aggregates. Thus, the lifetime of the excited

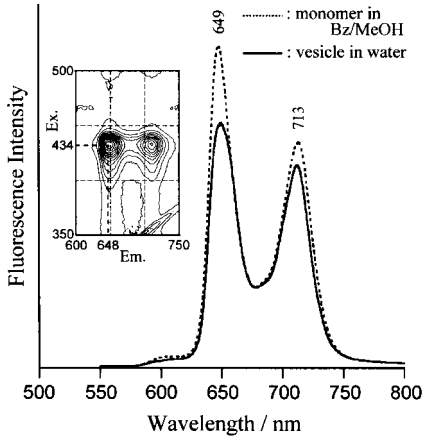

Figure 5. Fluorescence emission spectra of lipid-porphyrin **6a** (1.7 μM) at 25 °C (excitation at 428 nm). The inset shows emission–excitation correlation image.

singlet state of the vesicles (τ_F = 6.8 ns) was not dramatically different from that of the monomers (τ_F = 10 ns).

Laser flash photolysis experiments were carried out with nanosecond laser excitations. The transient absorption spectrum of the **6a** monomer in benzene/MeOH after laser flash illumination displayed the typical triplet–triplet (TT) absorption of TPP, in which the dark decay obeyed first-order kinetics (triplet lifetime τ_T = 2.0 ms) and is strongly accelerated by the presence of O_2 (Figure 6). Excitation of the **6a**

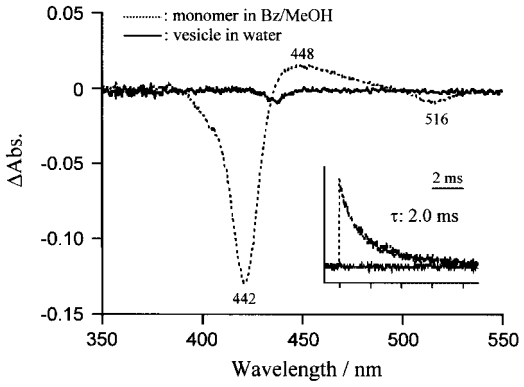

Figure 6. Transission–absorption differential spectra of lipid-porphyrin **6a** in solution 50 ns after laser-flash photolysis (excitation at 516 nm) under an Ar atmosphere ([**6a**] = 1.7 μM). The inset shows the absorption decay at 450 nm.

bilayer vesicles, on the other hand, gave small-magnitude signals with a lifetime that was too small to observe with our nanosecond instrumentation. If internal conversion is the only process influenced by self-assembly, the triplet state would be quenched to the same extent as the fluorescence, but this was not seen. These observations on the excited singlet and triplet

  0947-6539/02/0823-5473 $ 20.00+.50/0

states of the **6a** vesicles are almost the same as those on monolayered porphyrin platelets, which consist of laterally aligned porphyrins.[11h] Whitten et al. also reported a significant decrease in τ_T for 5,10,15,20-tetrakis(α^4-hexanamidophenyl)porphyrin J-aggregates in the presence of a small amount of surfactant in water.[20] There are two possible interpretations for the reduction of the triplet yield: 1) a decrease in the rate constant of intersystem crossing k_{isc}, and 2) an increase in the rate constant of triplet deactivation k_o. Based on our previous calculation for a similar porphyrin assembly,[11h] we can predict that the triplet lifetime of the **6a** vesicles may decrease by some 2 ns. The extremely short-lived triplet state of the lipid-porphyrin vesicles could be further evaluated using a picosecond laser flash apparatus.

Nanostructure of lipid-porphyrinatoiron assembly: The iron (III) complex of lipid-porphyrin **6b** also self-organizes in water to form spherical unilamellar vesicles with a diameter of 100 nm. The presence of a small excess of 1-dodecylimidazole (DIm, DIm/**6b** = 2.2 – 3.4 mol mol^{-1}) as an axial base did not hinder vesicle formation. The TEM of the evaporated **6b**/DIm solution on the copper grid showed an identical membrane with a thickness of 10 nm, which again corresponds to twice the length of the molecule (Figure 7). Light-scattering measurements gave a main diameter peak at 97 nm with a distribution of ±73 nm. The visible absorption spectrum (λ_{max} = 421, 570 nm) suggested the formation of a six-coordinate low-spin iron(III) complex with DIm ligands on both axial sites.

The aqueous **6b**/DIm was then transferred to highly oriented pyrolytic graphite (HOPG) and subjected to SFM under ambient conditions. The collapsed vesicles became detectable; they are obviously images of flattened **6b**/DIm assemblies on the graphite surface (Figure 7b). The thickness measured from the height profile of the evaporated vesicle was 19.5 nm (vertical distance a – a in Figure 7b), which corresponds to twice the thickness of the bilayer membrane. For evaluation of the lateral size, we should normally consider the horizontal broadening effect due to the shape of the tip, but this is not necessary for the vertical distance.[21] We can therefore conclude that the iron complex with DIm produces bilayer vesicle membranes, like free-base **6a**.

O_2 coordination to lipid-porphyrinatoiron(II) vesicles: The UV/Vis absorption spectrum of a phosphate buffer solution of the Fe^{II} **6c**/DIm vesicles revealed the presence a typical six-coordinate low-spin Fe^{II} species (λ_{max} = 436, 538, 568 nm) (Figure 8).[22] The TEM of the solution again exhibited spherical unilamellar vesicles with a wall of bilayer thickness (10 nm, not shown). Upon exposure of these vesicles to O_2 gas, the absorption spectrum immediately changed to that of an O_2 adduct (λ_{max} = 435, 543 nm). This dioxygen complex was kinetically stable in the wide range of 5 – 50 °C, depending on the O_2 partial pressure. Reversion of the O_2 adduct to the bis(DIm)-ligated species on bubbling N_2 gas was observed, that is, the dissociated DIm remains in the membrane interior during the dioxygenation and rebinds rapidly to the iron center after deoxygenation. The constant morphology of the vesicle throughout the reversible O_2 coordination cycle was

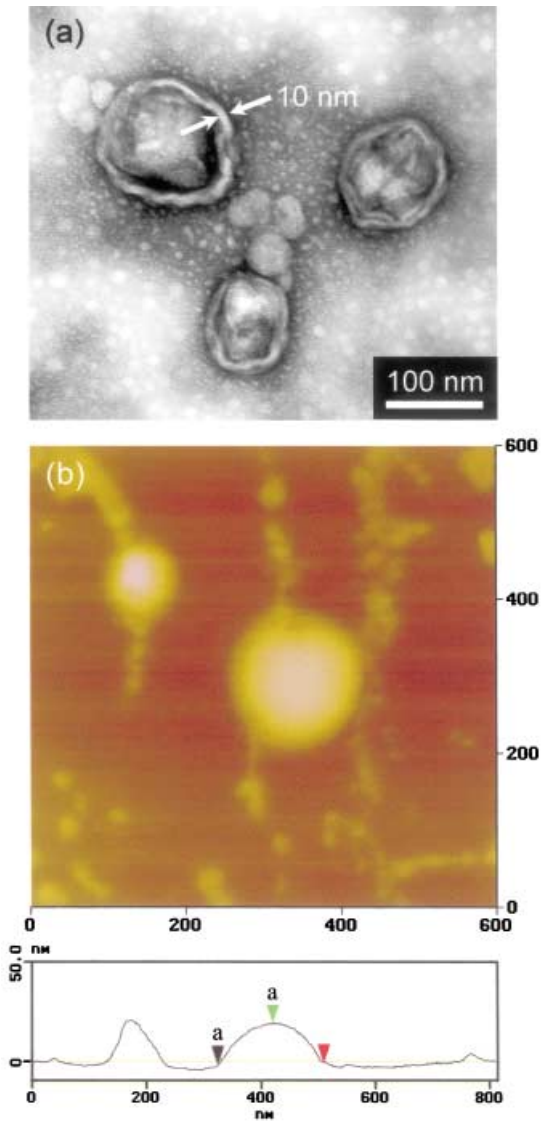

Figure 7. a) Transmission electron micrograph of vesicles of the lipid-porphyrinatoiron(III) complex **6b**/DIm negatively stained with uranyl acetate. b) SFM images (tapping mode) of the evaporated sample of **6b**/DIm vesicles on HOPG. Image size is 600 × 600 nm (z range: 50 nm), and its cursor profile 19.5 nm (vertical distance a – a).

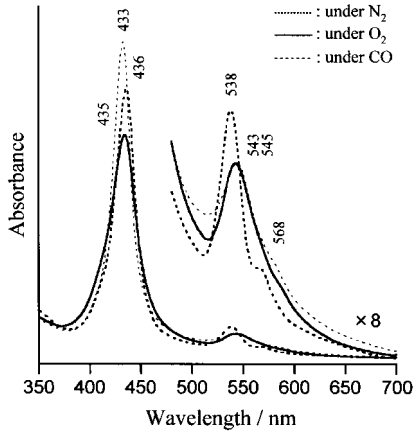

Figure 8. Visible absorption spectral changes for vesicles of the lipid-porphyrinatoiron(II) complex **6c**/DIm in phosphate buffer solution (pH 7.3) at 25 °C.

0947-6539/02/0823-5474 $ 20.00+.50/0 *Chem. Eur. J.* **2002**, *8*, No. 23

confirmed by TEM. Bubbling carbon monoxide into this solution gave the more stable carbonyl complex ($\lambda_{max} = 433$, 545 nm).

Oxidation to the Fe^{III} species was very slow; the half-life of the O_2 adduct was 17 h at 37 °C. The relationship between the O_2 binding ratio and O_2 pressure, that is, the O_2 equilibrium curve, was plotted on the basis of the UV/Vis absorption spectral changes on O_2 titration (Figure 9). The apparent O_2 binding affinity [$P_{1/2}$ is the gas pressure at half O_2 coordination of porphyrinatoiron(II)] of the **6c**/DIm vesicles was determined to be 30 Torr at 37 °C, a value similar to that of human erythrocytes.[23] Although the O_2-binding profile did not show any cooperativity like that seen in hemoglobin, their O_2-transporting efficiency between the lungs ($P_{O_2} = 110$ Torr) and muscle tissue ($P_{O_2} = 40$ Torr) is 20 %, which is nearly the same value (22 %) as that of human erythrocytes.

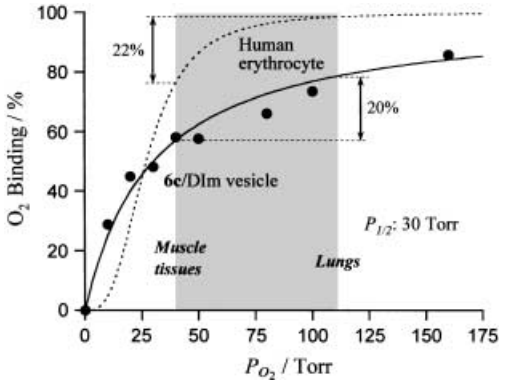

Figure 9. O_2 equiblium curve of vesicles of the lipid-porphyrinatoiron(II) complex **6c**/DIm in phosphate buffer solution (pH 7.3) at 37 °C.

Differential scanning calorimetry (DSC): The thermal behavior of the lipid-porphyrin bilayer membranes was studied by DSC. Three samples, **6a**, **6b**, and **6b**/DIm vesicles, demonstrated gel-phase (liquid-crystal) transitions (Table 1). Free

Table 1. Phase transition temperatures of the lipid-porphyrin vesicles and their thermodynamic parameters.

System	T_c [°C]	ΔH [kcal mol^{-1}]	ΔS [cal mol^{-1}deg^{-1}][a]	ΔS_{CH_2} [cal mol^{-1}deg^{-1}]
6a	56	4.1	73.2	0.54
6b	49	3.7	75.5	0.56
6b/DIm	40	1.5	29.4	–
DPPC[b]	41	8.6	27.3	0.90

[a] $\Delta S = \Delta H T_c^{-1}$. [b] DPPC = 1,2-diparmytoyl-*sn*-glycero-3-phosphatidylcholine.[24]

base **6a** showed a relatively sharp transition at 56 °C with an enthalpy change ΔH of 4.1 kcal mol^{-1}; this suggests that the long acyl chains on the porphyrin are responsible for formation of close-packed layers. We are certain that the trimethylolethane residue in the lipid group plays the same role as a glycerol residue. It is remarkable that the ferric complex **6b** had a lower phase-transition temperature T_c of 49 °C. This decrease may result from the different geometric alignments of the TPP planes in the membrane. As described above, free-base TPP forms triclinic crystals in which each porphyrin array shows a parallel arrangement of the nearest neighbor phenyl groups and a constant repeat distance. The stacking of all the phenyl rings is expected to provide some lattice stabilization. By contrast, the Fe^{III}–TPP complex aligns in a random conformation.[17] The porphyrin moieties in the **6a** bilayer are presumably oriented in a fashion similar to that in the free-base TPP crystal, which may afford additional stabilization to the membrane packing. Indeed, the temperature dependence of the absorption spectrum of the **6a** vesicles showed a small hypsochromic shift with broadening and a decrease in intensity at T_c (56 °C; Figure 10). This was observed only for the free-base **6a** porphyrin vesicles, and not for the iron complex.

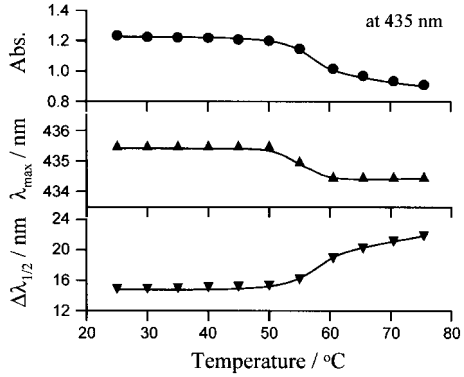

Figure 10. Temperature dependence of the Soret band absorption λ_{max} and half-width $\Delta\lambda_{1/2}$ of vesicles of the lipid-porphyrin **6a** in water.

Although the lipid-porphyrin vesicles have distinct phase transitions, their low ΔH values mean the alkyl chains are less dense than those of a 1,2-diparmytoyl-*sn*-glycero-3-phosphatidylcholine (DPPC) membrane. The increased amount of entropy per methylene unit (ΔS_{CH_2}), which is often used to evaluate the molecular packing (0.90 for DPPC),[24] was also low (0.54 and 0.56 for the **6a** and **6b** vesicles, respectively). The thermotropic characteristics of the iron-complex vesicles were further altered by addition of DIm, which resulted in a significant decrease in T_c and a drop of 2.2 kcal mol^{-1} in the enthalpy change of the transition.

Magnetic circular dichroism (MCD) and IR spectroscopy: For porphyrins and hemoproteins, MCD is a sensitive probe for oxidation state, spin state, and axial ligation of the metal center. It has been therefore used as a fingerprint for the coordination structure of various model hemes.[25] We applied the MCD and IR spectroscopy to characterize the O_2 adduct of the self-organized **6c**/DIm vesicles. Under an N_2 atmosphere, the MCD showed a well-characterized spectrum of bis(imidazole)-ligated six-coordinate low-spin Fe^{II} porphyrin, which differs strongly to that of a five-coordinate high-spin complex with mono-imidazole ligation (Figure 11). This observation indicates that axial coordination is not affected by the dense packing of the four phospholipid groups on the porphyrin plane. Admission of O_2 gas yields the six-coordinate **6c**/DIm(O_2) complex, which shows an S-shaped A-term MCD in the Soret region, as observed in the spectra of other dioxygenated Fe^{II}TPP derivatives.[25] The CO adduct is also

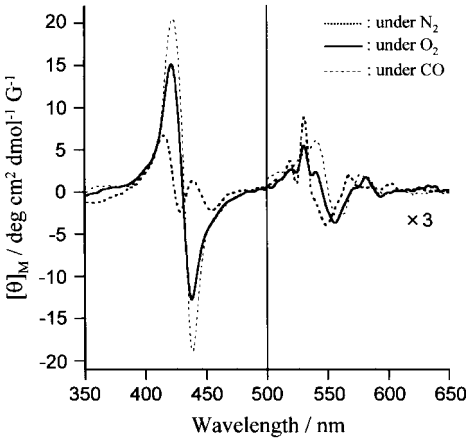

Figure 11. MCD spectra of vesicles of the lipid-porphyrinatoiron(II) complex **6c**/DIm in phosphate buffer solution (pH 7.3) at 25 °C.

low-spin and is expected to show a similar A-term MCD band with strong intensity; such a band was actually observed. In all cases, the complicated pattern in the Q-band regions coincided well with those previously reported (Table 2).[25]

Table 2. Absorption maxima of MCD spectra of the **6c**/DIm vesicles in phosphate buffer solution (pH 7.3) at 25 °C.

Atmosphere	MCD λ_{max} [nm]
N_2	416(+), 429(−), 439(+), 454(−), 519(+) 531(+), 537(−), 549(−), 568(+), 574(−)
O_2	421(+), 438(−), 531(+), 541(+) 555(−), 572(+), 581(+), 593(−)
CO	422(+), 438(−), 538(+), 543(+) 557(−), 578(+), 545(−)

Difference IR spectra in solution of **6c**/DIm vesicles for CO versus $^{16}O_2$ complexes displayed a distinct positive band at the stretching frequency of coordinated CO at 1969 cm^{-1} (Table 3). In the spectrum for the $^{16}O_2$ versus the $^{18}O_2$ adduct, we

Table 3. IR spectral data of vesicles of the lipid-porphyrinatoiron(II) complex **6c**/DIm in phosphate buffer solution (pH 7.3) at 25 °C.

System	$\nu(^{16}O-^{16}O)$	$\nu(^{18}O-^{18}O)$	$\nu(^{12}C-^{16}O)$
6c/DIm vesicles	1155	1081	1969
$FeT_{piv}PP/MIm$[a]	1159	1075	1969
hemoglobin[27]	1107	1065	1951
O_2 or CO gas	1556	–	2143
O_2^-	1145	–	–

[a] $FeT_{piv}PP/MIm$ = 5,10,15,20-Tetrakis(*α*,*α*,*α*,*α*-*o*-pivalamidophenyl)porphyrinatoiron(II) – 1-methylimidazole complex.[26]

observed the appearance of a positive band at 1155 cm^{-1} and a negative peak at 1081 cm^{-1}, both of which correspond to the stretching frequencies of the coordinated O_2 molecules. The frequency shifts between $^{16}O_2$ and $^{18}O_2$ adducts (74 cm^{-1}) is in good agreement with the value calculated from the harmonic-oscillator prediction of the O–O stretching vibration. Their ν(O–O) bands are close to not only those of ionic superoxides, but also to those of the bent end-on O_2 bound to other synthetic Fe^{II}TPP systems in benzene or Nujol.[26] On the basis of these findings, we conclude that the self-organized **6c** bilayer vesicles coordinate molecular O_2 like hemoglobin and model hemes,[26, 27] without any hinderance by aggregation.

Conclusion

The synthesized lipid-porphyrins are giant porphyrin amphiphiles with the ability to form perfectly round bilayer vesicles in aqueous solution. The glycerol in the phospholipids can be replaced by trimethylolethane. Indeed, phospholipids in which trimethylolethane residues links diparmytoyl chains and phosphocholine head group assemble in water to give unilamellar vesicles similar to those formed by DPPC.[28] The advantages of the trimethylolethane-based approach are: 1) the synthetic procedures to connect the acyl chains are easier than with glycerol, as shown in this work; and 2) the two acyl groups are bound in a symmetric form, which is not realized in natural lecithin.[29] This could give parallel geometric arrays of alkyl chains in membrane layers. For instance, for radical polymerization of unsaturated lipids, the double bonds oriented side by side will provide high polymerization yields. In the interior of the lipid-porphyrin vesicle, two sheets made of J-aggregated TPP planes presumably stack with a lateral displacement. Exciton coupling theory confirmed our predicted models, which is similar to that seen in the triclinic unit cell of free-base TPP crystals, except for the slightly wider interlayer distance (ca. 6.0 Å), and it reproduced the Soret band bathochromic shifts in the visible absorption of the **6a** vesicles. The free-base lipid-porphyrin bilayers form a strongly fluorescent aggregate, but show an extraordinarily short triplet lifetime. We consider that this unique photophysical behavior is due to the edge-to-edge alignment of the porphyrin platforms. Furthermore, the N-coordinated high-spin Fe^{II} complex **6c**/DIm membranes can bind one equivalent of O_2 molecules. An aqueous solution of the **6c**/DIm vesicles with high concentration (>mM) is an entirely synthetic O_2 carrier that could act as a substitute for red blood cells. These bilayer membranes possess a spherical architecture consisting of 23 000 porphyrins in water, and are a new class of a supramolecular assembly that can realize important biological reactions of porphyrinoids in nature: not only O_2 transport, but also metabolic oxidation and photo-induced electron or energy transfer. In particular, there has been substantial recent interest in the construction of cyclic multiporphyrin assemblies, since a wheel-shaped bacteriochlorophyll circuit has been found in a light-harvesting antenna complex.[30] More recently, we have prepared multicomponent vesicles made of differently metalated lipid-porphyrins, in which efficient energy transfer due to the tightest packing of the chromophores is observed. A new investigation of the photoinduced electronic communication in the lipid-porphyrin architecture is underway.

Experimental Section

Materials and apparatus: All commercially available reagents of high-purity grades were used without further purification, unless otherwise

0947-6539/02/0823-5476 $ 20.00+.50/0 *Chem. Eur. J.* **2002**, *8*, No. 23

stated. Solvents were normally purified by distillation before use. Dichloromethane was refluxed over and distilled from P_2O_5. Tetrahydrofuran was refluxed over and distilled from sodium wire. Water was deionized by using an ADVANTEC GS-200 system. Thin-layer chromatography (TLC) was carried out on 0.2 mm precoated plates of silica gel 60 F_{254} (Merck). Purification was performed by column chromatography on silica gel (Merck, Keiselgel 60, Art 7736) or Sephadex LH-60 gel (Amersham Pharmacia Biotech). Infrared spectra were recorded on a JASCO FT/IR-410 spectrometer. ^{1}H NMR spectra were measured on a JEOL Lambda 500 spectrometer (500 MHz), and chemical shifts are expressed in parts per million downfield from Me_4Si as internal standard. FAB-MS spectra were obtained on a JEOL JMS-SX102A spectrometer. Elemental analysis was performed on a Yanagimoto MT3 CHN corder. UV/Vis absorption spectra were recorded on a JASCO V-570 spectrophotometer, and steady-state fluorescence spectra on a HITACHI F-4500 spectrofluorometer. Magnetic circular dichroism spectra were obtained on a JASCO J-820 spectropolarimeter. Light-scattering measurements were performed on a COULTER Model N4SD. All these measurements were normally carried out at 25 °C. 5,10,15,20-Tetrakis[*α*,*α*,*α*,*α*-*o*-(2,2-dimethyl-20-hydroxyicosanamido)phenyl]porphine [TPP-(C_{18}OH)$_4$] and 2-chloro-1,3,2-dioxaphospholane 2-oxide were prepared according to the previously reported procedures.[13]

2,2-Bis(hydroxymethyl)-1-trityloxypropane (1): A solution of trityl chloride (13 g, 46.6 mmol) in dry DMF (150 mL) was added dropwise over about 90 min to a solution of 2-hydroxymethyl-2-methyl-1,3-propanediol (6.0 g, 50 mmol) and pyridine (8.4 mL) in dry DMF (24 mL) at 85 °C under an N_2 atmosphere. Then the mixture was stirred for a further 3 h at 95 °C. The DMF and pyridine were removed in vacuo, and the residue was extracted with $CHCl_3$ and washed with water. The organic layer was dried over anhydrous Na_2SO_4 and the solvent was evaporated. Excess methanol was then poured into the mixture, and the resulting precipitate was filtered off. The mother liquor was again evaporated. The product was separated by column chromatography on silica gel with $CHCl_3$/MeOH (10:1) as eluent. The major band was collected and dried at room temperature for several hours in vacuo to give compound **1** as a viscous solid (3.37 g, 19 %). R_f = 0.40 ($CHCl_3$/MeOH, 10:1); IR (NaCl): $\tilde{\nu}$ = 1154 (COC, ether), 3390 cm^{-1} (OH, alcohol); ^{1}H NMR (500 MHz, $CDCl_3$, 25 °C, TMS): δ = 0.9 (s, 3H; CH_3), 3.0 (s, 2H; CH_2OTri), 3.5 (s, 4H; CH_2OH), 7.2 – 7.4 ppm (m, 15H; Tri). MS: *m*/*z* calcd for $C_{24}H_{26}O_3$: 362.19; found: 362.26 [M^+].

2-Hydroxymethyl-2-octadecanoyloxymethyl-1-trityloxypropane (2): Compound **1** (3.37g, 9.30 mmol), stearic acid anhydride (5.12 g, 9.30 mmol), and 4-DMAP (568 mg, 4.65 mmol) were dissolved in dry THF (100 mL), and the solution was refluxed for 12 h under an N_2 atmosphere. After evaporation of the solvent, excess methanol was added, and a white precipitate was removed. The mother liquor was evaporated and the resulting mixture was separated by column chromatography on silica gel with $CHCl_3$/Et_2O (30:1) as eluent. The major band was collected and dried at room temperature for several hours in vacuo to give compound **2** as a viscous liquid (3.67 g, 63 %). R_f = 0.50 ($CHCl_3$/Et_2O, 30:1); IR (NaCl): $\tilde{\nu}$ = 1176 (COC, ether), 1737 (C=O, ester), 3490 cm^{-1} (OH, alcohol); ^{1}H NMR (500 MHz, $CDCl_3$, 25 °C, TMS): δ = 0.8 (t, 3H; $(CH_2)_{16}CH_3$), 0.9 (s, 3H; CH_3), 1.3 (s, 28H; $(CH_2)_{14}CH_3$), 1.6 (m, 2H; C(=O)CH_2CH_2), 2.3 (t, 2H; C(=O)CH_2), 3.1(q, 2H; CH_2OTri), 3.5 (q, 2H; CH_2OH), 4.2 (q, 2H; CH_2OC(=O)), 7.2 – 7.5 ppm (m, 15H; Tri). MS: *m*/*z* calcd for $C_{42}H_{60}O_4$: 628.45; found: 627.5 [M^+ – H].

2-(3-Carboxypropanoyloxy)methyl-2-octadecanoyloxymethyl-1-trityloxypropane (3): A solution of **2** (3.67 g, 5.85 mmol), succinic acid anhydride (4.09 g, 40.9 mmol), and 4-DMAP (1.43 g, 11.7 mmol) in dry THF (170 mL) was refluxed for 12 h under an N_2 atmosphere. The resulting mixture was brought to dryness on a rotary evaporator and extracted with $CHCl_3$. The organic layer was washed with water and dried over anhydrous Na_2SO_4. The solvent was then evaporated, and the residue was separated by column chromatography on silica gel with $CHCl_3$/MeOH (20:1) as eluent. The major band was collected and dried at room temperature for several hours in vacuo to give compound **3** as a white solid (3.42 g, 83 %). R_f = 0.45 ($CHCl_3$/MeOH, 20:1); IR (NaCl): $\tilde{\nu}$ = 1160 (COC, ether), 1714 (C=O, carboxyl), 1741 cm^{-1} (C=O, ester); ^{1}H NMR (500 MHz, $CDCl_3$, 25 °C, TMS): δ = 0.9 (t, 3H; $(CH_2)_{16}CH_3$), 1.0 (s, 3H; CH_3), 1.3 (s, 28H; $(CH_2)_{14}CH_3$), 1.6 (m, 2H; C(=O)$CH_2CH_2(CH_2)_{14}$), 2.2 (t, 2H; OC(=O)$CH_2(CH_2)_{15}$), 2.6 (m, 4H; $(CH_2)_2$COOH), 3.1 (s, 2H; CH_2OTri), 4.2 (d, 4H; CH_2OC(=O)), 7.3 – 7.5 ppm (m, 15H; Tri). MS: *m*/*z* calcd for $C_{46}H_{64}O_7$: 728.47; found: 751.53 [M^++Na].

5,10,15,20-Tetrakis{*α*,*α*,*α*,*α*-*o*-{20-[3-(2-octadecanoyloxymethyl-2-trityloxymethylpropanoxycarbonyl)propanoyloxy]-2,2-dimethylicosanamido}phenyl}porphine (4): TPP-(C_{18}OH)$_4$[13] (607 mg, 0.299 mmol) was added to a solution of **3** (2.4 g, 1.19 mol), DCC (676 mg, 3.27 mmol), and 4-DMAP (182 mg, 0.3 mmol) in dry CH_2Cl_2 (25 mL). The mixture was stirred for 20 h at room temperature in darkness. After evaporation of CH_2Cl_2, the residue was redissolved in benzene, and the undissolved white DC urea was removed by filtration. The mother liquor was brought to dryness on a rotary evaporator. Then a $CHCl_3$ solution of the obtained porphyrin was added dropwise to excess MeOH to give a purple precipitate. The filtered crude porphyrin was finally purified by column chromatography on silica gel with $CHCl_3$/Et_2O (30:1) as eluent. The main band was collected and dried at room temperature for several hours in vacuo to give compound **4** as a purple solid (1.36 g, 94 %). R_f = 0.50 ($CHCl_3$/Et_2O, 30:1); IR (NaCl): $\tilde{\nu}$ = 1156 (COC, ether), 1692 (C=O, amide), 1739 (C=O, ester), 3437 cm^{-1} (NH, amide); UV/Vis ($CHCl_3$): λ_{max} = 419, 513, 545, 587, 642 nm; ^{1}H NMR (500 MHz, $CDCl_3$, 25 °C, TMS): δ = – 2.6 (s, 2H; inner H), – 0.2 (s, 24H; 2,2-dimethyl), 0.8 (t, 12H; $(CH_2)_{16}CH_3$), 1.0 (s, 12H; CH_3), 1.0 – 1.3 (m, 112H; $(CH_2)_{14}CH_3$, 128H; $(CH_2)_{16}$), 1.5 (m, 8H; OC(=O)$CH_2CH_2(CH_2)_{14}$, 8H; CH_2CH_2OC(=O)), 2.2 (t, 8H; OC(=O)$CH_2(CH_2)_{14}$), 2.5 (s, 16H; OC(=O)$(CH_2)_2$C(=O)O), 3.0 (m, 8H; CH_2OTri), 4.0 (m, 16H; C(CH_2OC(=O))$_2$, 8H; CH_2OC(=O)$(CH_2)_2$), 7.1 (s, 4H; amide), 7.2 – 7.3 (m, 60H; Tri), 7.4 (t, 4H; Ph H4), 7.7 (t, 8H; Ph H5), 7.8 (d, 4H; phenyl H3), 8.7 (d, 4H; Ph H6), 8.8 ppm (s, 8H; pyrrole).

5,10,15,20-Tetrakis{*α*,*α*,*α*,*α*-*o*-{20-[3-(2-octadecanoyloxymethyl-2-hydroxymethylpropanoxycarbonyl)propanoyloxy]-2,2-dimethylicosanamido}phenyl}porphine (5a): Boron trifluoride methanol complex (0.85 mL, 1.64 mmol) was added to a solution of **4** (1.33 g, 0.273 mmol) in dry CH_2Cl_2 (60 mL). After stirring for 4 h at room temperature, the green solution was carefully poured into ice/water to stop the reaction, and the mixture extracted with $CHCl_3$. The organic layer was dried over anhydrous Na_2SO_4 and evaporated. Then a $CHCl_3$ solution of the residue was added dropwise to the excess MeOH to precipitate the porphyrin. The filtered crude product was purified by column chromatography on silica gel with $CHCl_3$/MeOH (20:1) as eluent. The major fraction was collected and dried at room temperature for several hours in vacuo to give compound **5a** as a purple solid (1.07 g, 92 %). R_f = 0.3 – 0.4 ($CHCl_3$/MeOH, 20:1); IR (NaCl): $\tilde{\nu}$ = 1691 (C=O, amide), 1738 (C=O, ester), 3436 (NH, amide), 3502 cm^{-1} (OH, alcohol); UV/Vis ($CHCl_3$): λ_{max} = 419, 513, 545, 587, 642 nm; ^{1}H NMR (500 MHz, $CDCl_3$, 25 °C, TMS): δ = – 2.6 (s, 2H; inner H), – 0.2 (s, 24H; 2,2-dimethyl), 0.8 (t, 12H; $(CH_2)_{16}CH_3$), 1.0 (s, 12H; CH_3), 1.0 – 1.3 (m, 112H; $(CH_2)_{14}CH_3$, 128H; $(CH_2)_{16}$), 1.7 (m, 8H; OC(=O)$CH_2CH_2(CH_2)_{14}$, 8H; CH_2CH_2OC(=O)), 2.3 (t, 8H; OC(=O)$CH_2(CH_2)_{14}$), 2.6 (s, 16H; OC(=O)$(CH_2)_2$C(=O)O), 3.4 (d, 8H; CH_2OH), 4.1 (m, 16H; C(CH_2OC(=O))$_2$, 8H; CH_2OC(=O)$(CH_2)_2$), 7.1 (s, 4H; amide), 7.5 (t, 4H; Ph H4), 7.8 (t, 8H; Ph H5), 7.9 (d, 4H; Ph H3), 8.7 (d, 4H; Ph H6), 8.8 ppm (s, 8H; pyrrole); elemental analysis calcd (%) for $C_{240}H_{394}N_8O_{32}\cdot C_6H_6$ (3981.9): C 74.20, H 10.12, N 2.81; found: C 74.34, H 9.72, N 2.71.

Iron complex of 5a (5b): A solution of **5a** (296 mg, 75.9 μmol) and 2,6-lutidine (62.5 μL) in dry THF (40 mL) was added dropwise to anhydrous $FeBr_2$ (0.7 g) under dry N_2. The mixture was refluxed for 2 h under an N_2 atmosphere. The resulting solution was brought to dryness, and the residue was extracted with $CHCl_3$ and washed with water. After drying over anhydrous Na_2SO_4, the organic layer was evaporated, and the crude compound was separated by column chromatography on silica gel with $CHCl_3$/MeOH (20:1) as eluent. The major band was collected and dried at room temperature for several hours in vacuo to give compound **5b** as dark purple solid (249 mg, 81 %). R_f = 0.2 – 0.3 ($CHCl_3$/MeOH, 20:1); IR (NaCl): $\tilde{\nu}$ = 1692 (C=O, amide), 1737 (C=O, ester), 3433 (NH, amide), 3460 cm^{-1} (OH, alcohol); UV/Vis ($CHCl_3$): λ_{max} = 357, 417, 506, 577, 644, 683 nm.

5,10,15,20-Tetrakis{*α*,*α*,*α*,*α*-*o*-{20-[3-(2-octadecanoyloxymethyl-2-trimethylammonioethoxyphosphonatoxymethylpropanoxycarbonyl)propanoyloxy]-2,2-dimethylicosanamido}phenyl}porphinatoiron(III) bromide (6b): 2-Chloro-1,3,2-dioxaphospholane 2-oxide (372 μL) was added to a solution of **5b** (249 mg, 61.6 μmol) and triethylamine (0.637 mL, 4.58 mmol) in dry CH_2Cl_2 (20 mL) at 0 °C under an argon atmosphere. After stirring the mixture for 1 h and an additional 1 h at room temperature, the solvent was removed under reduced pressure. Then, the resultant phosphate triester was redisolved in dry DMF (30 mL), and anhydrous trimethylamine

(4.0 mL) was immediately added. The mixture was sealed in a pressure bottle and allowed to react for 1 h at room temperature. After an additional 16 h at 60 °C, the solvent was removed, and the residue was washed with MeOH. The remaining brown crude porphyrin was purified by gel column chromatography on Sephadex LH-60 with benzene/MeOH (2:1) as eluent to give a compound **6b** as dark purple solid (202 mg, 79 %). IR (NaCl): $\tilde{\nu}$ = 1087 (POC, phosphate), 1216 (P=O, phosphate), 1692 (C=O, amide), 1735 (C=O, ester), 3431 cm^{-1} (NH, amide); UV/Vis ($CHCl_3$): λ_{max} = 353, 417, 501, 574, 635, 680 nm; elemental analysis calcd (%) for $C_{260}H_{440}N_{12}O_{44}P_4$·FeBr $2H_2O$ (4734.07): C 65.97, H 9.45, N 3.55; found: C 66.23, H 9.46, N 3.18.

Free-base porphyrin (6a): Phosphocholine groups were introduced into compound **5a** by using the same procedure as for **6b** (Yield: 80 %). IR (NaCl): $\tilde{\nu}$ = 1089 (POC, phosphate), 1236 (P=O, phosphate), 1692 (C=O, amide), 1734 (C=O, ester), 3430 cm^{-1} (NH, amide); UV/Vis ($CHCl_3$): λ_{max} = 422, 516, 549, 590, 646 nm; ^{1}H NMR (500 MHz, $CDCl_3/CD_3OD$, 25 °C, TMS): δ = −2.6 (s, 2H; inner H), −0.4 (s, 24H; 2,2-dimethyl), 0.7 (t, 12H; $(CH_2)_{16}CH_3$), 0.8 (s, 12H; CH_3), 0.8–1.2 (m, 112H; $(CH_2)_{14}CH_3$, 128H; $(CH_2)_{16}$), 1.4 (m, 8H; $OC(=O)CH_2CH_2(CH_2)_{14}$, 8H; $CH_2CH_2OC(=O)$), 2.1 (t, 8H; $OC(=O)CH_2(CH_2)_{14}$), 2.4 (s, 16H; $OC(=O)(CH_2)_2C(=O)O$), 3.0 (s, 36H; $N^+(CH_3)_3$), 3.4 (t, 8H; $CH_2N^+(CH_3)_3$), 3.6 (s, 8H; $P(=O)OCH_2$), 3.8 (m, 16H; $C(CH_2OC(=O))_2$, 8H; $CH_2OC(=O)(CH_2)_2$), 4.0 (t, 8H; $CH_2CH_2N^+(CH_3)_3$), 7.1 (s, 4H; amide), 7.3 (t, 4H; Ph H4), 7.6 (t, 8H; Ph H5), 7.7 (d, 4H; Ph H3), 8.4 (d, 4H; Ph H6), 8.6 ppm (s, 8H; pyrrole).

Preparation of aqueous lipid-porphyrin solutions

Free-base lipid-porphyrin solution: A benzene/methanol stock solution of **6a** (50 μL, 2.0 mM) was placed in a 5 mL round bottom flask and slowly evaporated on a rotary evaporator under reduced pressure to give a thin film of the porphyrin at the bottom. The film was then dried in vacuo for 3 h; deionized water (5 mL) heated to 60 °C was then injected. The mixture was homogenized by vortex mixing with several small glass beads (ca. 10) and briefly ultrasonicated by a bath-type sonicator. The resulting red solution (20 μM) was incubated for at least 12 h at room temperature before use.

Lipid-porphyrinatoiron(II) solution. A benzene/methanol stock solution of **6b** (50 μL, 2.0 mM) and a solution of 1-dodecylimidazole in $CHCl_3$ (110–165 μL, 2.0 mM) was slowly evaporated by using a rotary evaporator, as described above, to give a thin film at the bottom of the flask. The film was dried in vacuo for 3 h, and phosphate buffer (pH 7.3, 1 mM, 5 mL) heated at 60 °C was added. Homogenization by a tip-type ultrasonicator (60 mW, 3 min) in a water bath gave a yellow-brown solution, which was incubated for at least 12 h at room temperature. Then the **6b** solution (20 μM) was deaerated by N_2 bubbling; addition of aqueous sodium dithionate (15 mM, 20 μL) gave a solution of the bis-imidazole iron(II) complex **6c**. Excess sodium dithionate was removed by quick passage through a Sephadex G-25 (coarse) column.

Transmission electron microscopy (TEM): The negatively stained specimens for TEM were prepared as in previously reported procedures.[11f] The grids were observed in a JEOL JEM-100CX electron microscope at an accelerating voltage of 100 kV.

Scanning force microscopy (SFM): A droplet of porphyrin solution (1–5 μM) was pipetted onto freshly cleaved, highly oriented pyrolytic graphite (HOPG STM-1, Advanced Ceramics Co.). After 1 min, excess fluid was carefully blotted off by filter paper, and air-drying was carried out for a further 1 h. SFM measurements were carried out on a Nanoscope III system (Digital Instruments Inc.) in the tapping mode under ambient laboratory conditions. Silicon cantilevers (length 125 μm) with a spring constant between 21 and 78 $N\,m^{-1}$ and a resonance frequency in the range 260–410 kHz were used. The scanning rate was usually 1.0 Hz. Imaging was simultaneously performed by displaying the amplitude signal and the height signal.

Langmuir–Blodgett layer and Π–A isotherm: A monolayer of lipid-porhyrin was prepared at the air/water interface in a Nippon Laser & Electronics LB Film Deposition System. Compound **6a** was spread from a 1.17 mM solution in $CHCl_3$/MeOH (10:1) onto the pure water subphase. The area per **6a** molecule was estimated from its surface pressure versus molecular area (Π–A) isotherm. Furthermore, the monolayer was pulled onto a clean glass plate to give a lipid-porphyrin monolayer, which was applied perpendicular to the monolayer surface and slowly pulled up to give porphyrin trilayers.

Exciton calculation

Monolayer: The center-to-center distance r_{mn} of the dipole moments between the origin porphyrin P_o and the neighbor P_{mn} (Figure 4c) is given by Equation (2)

$$r_{mn} = [(ma)^2 + (nb)^2]^{1/2} \quad (2)$$

the angle θ_{mn} by Equation (3)

$$\tan\theta_{mn} = nb/ma \quad (3)$$

and the exciton interaction energies V_{mn} for the S_x transitions and V'_{mn} for the S_y transitions by Equations (4) and (5).

$$V_{mn} = M^2 r_{mn}^{-3}(1 - 3\cos^2\theta_{mn}) \quad (4)$$

$$V'_{mn} = M^2 r_{mn}^{-3}(1 - 3\sin^2\theta_{mn}) \quad (5)$$

The total energy is the sum of the interactions of the infinite porphyrin alignments on the 22 lines crossing the origin of the coordinate axes: V for the S_x transitions and the V' for the S_y transitions.

Bilayer: The core of the porphyrin P_{kl} in the upper layer is assumed to be shifted by +4.02, +2.68, and +d Å in the x, y, and z directions, respectively, from the center of the nearest porphyrin P_{mn} in the layer below. The center-to-center distance r_{kl} of the dipole moments between porphyrin P_o and each porphyrin P_{kl} is given by Equation (6).

$$r_{kl} = [(ma + 4.02)^2 + (nb + 2.68)^2 + d^2]^{1/2} \quad (6)$$

The angles θ_{kl} for the S_x transitions and θ'_{kl} for the S_y transitions are are given by Equations (7) and (8).

$$\cos\theta_{kl} = (ma + 4.02)r_{kl}^{-3} \quad (7)$$

$$\cos\theta'_{kl} = (nb + 2.68)r_{kl}^{-3} \quad (8)$$

The exciton interaction energy V_{kl} for the S_x transitions and V'_{kl} for the S_y transitions is given by Equations (9) and (10).

$$V_{kl} = M^2 r_{kl}^{-3}(1 - 3\cos^2\theta_{kl}) \quad (9)$$

$$V'_{kl} = M^2 r_{kl}^{-3}(1 - 3\cos^2\theta'_{kl}) \quad (10)$$

The total energy is the sum of the interactions between P_o and 46 porphyrins on the upper layer within a circle of about 5 nm: V_I for the S_x transitions and V'_I for the S_y transitions. Then the overall excitonic interaction in our bilayer model is finally defined as the sum of V and V_I for the S_x transitions and V' and V'_I for the S_y transitions.

Excited-state lifetimes: Singlet lifetimes of **6a** were measured by using a Horiba NAES-500 nanosecond fluorometer with an N_2 lamp (excitation-side band-path filter: MC560, emission-side color filter: R62). The samples were held in a cuvette (optical path length 1 cm). Triplet lifetime measurements on the nanosecond timescale were performed by using a Unisoku TSP-600 time-resolved spectrophotometer system with a Continuum Surelite I-10 Q-switched Nd:YAG laser, which generated a second-harmonic (532 nm) pulse of 6 ns duration with an energy of 200 mJ per pulse (10 Hz). A 150 W Xenon arc lamp was used as the monitor light source. The triplet decay of **6a** was monitored by transient absorption at 450 nm. The concentration of the lipid-porphyrin was 1.7 μM, and experiments were carried out at 25 °C. Time-resolved transient absorption spectra after nanosecond laser flash photolysis were measured by an ANDOR DH520-18F-WR ICCD detector with an ORIEL MS-257 imaging monochromator. The excitation laser pulse with a wavelength of 516 nm was generated from the THG (355 nm; pulse width, 5 ns) of a Spectron SL803G-10 Nd:YAG laser by using a GWU BBO-OPO photoparametric oscilator. A pulsed xenon flash lamp (10 W, 10 Hz, 100 ns pulse width) was used as the monitor light source. The path length of the cuvette was 10 mm, and all measurements were carried out by a Tokyo Instruments two-channel simultaneous detection system at 25 °C.

0947-6539/02/0823-5478 $ 20.00+.50/0 *Chem. Eur. J.* **2002**, *8*, No. 23

O_2 Binding: O_2-binding to the lipid-porphyrinatoiron(II) complex is expressed by Equation (11):

$$FeLP + O_2 \rightleftharpoons FeLP-O_2 \quad (11)$$

where FeLP is lipid-porphyrinatoiron(II) complex **6c**. The apparent O_2-binding affinity (gaseous pressure at half O_2 binding for **6c**, $P_{1/2}$) was determined by spectral changes at various partial pressure of O_2, as described in the literature.[12] The half-life of the dioxygenated species was determined by the time dependence of the absorption intensity at 540 nm, which is due to the O_2 adduct.

Magnetic circular dichroism (MCD): MCD was measured on a phosphate buffer solution of **6c**/DIm vesicles (8.0 μM) under N_2, CO, and O_2 atmospheres on a JASCO J-820 circular dichrometer fitted with a 1.5 T electromagnet. The accumulations were normally two performed twice, and from each datum the value without an electromagnetic field was subtracted as baseline.

Infrared spectroscopy: The phosphate buffer (pH 7.3, 1 mM) solution of **6c** vesicles (3 mM) containing three equivalents of DIm was prepared by a procedure similar to that described above in a bath-type ultrasonic generator, followed by reduction with sodium dithionate. Separate samples of this solution were exposed to atmospheres of CO, $^{16}O_2$, and $^{18}O_2$ (ISOTEC Inc., 99% enriched). Infrared spectra of each solution were measured between 2000 and 1000 cm^{-1} on a JASCO FT/IR-410 spectrometer at 4 cm^{-1} resolution. A CaF_2 cell (path length: 0.025 mm) was used for all measurements.

Differential scanning calorimetry (DSC): Aqueous solutions of **6a**, **6b**, and **6b**/DIm vesicles (1 wt%) were prepared by the same procedure as for IR measurements. DSC for all samples was measured on a SEIKO Instruments DSC120 differential scanning calorimeter at a scan rate of 2 °C min^{-1} in the temperature range 5–80 °C.

Acknowledgements

We thank Prof. Naoki Yoshioka and Prof. Hidenari Inoue, Keio University (Yokohama) for the LB measurements, and JASCO Corporation for the use of the MCD spectrometers. This work was partially supported by Health Science Research Grants (Artificial Blood Project) of the Ministry of Health, Labor and Welfare and by a Grant-in-Aid for Scientific Research (No. 13650938) from the Ministry of Education, Culture, Sports, Science and Technology.

[1] J. K. M. Sanders in *Comprehensive Supramolecular Chemistry*, *Templating*, *Self-assembly*, *and Self-organization*, *Vol. 9* (Eds.: J.-M. Lehn, J. L. Atwood, J. E. D. Davies, D. D. MacNicol, F. Vögtle), Pergamon, Oxford, **1996**, pp. 131–164, and reference therein.

[2] Examples of multiporphyrinic assemblies of more than three porphyrin units in organic solvents: a) A. M. Brun, S. J. Atherton, A. Harriman, V. Heitz, J.-P. Sauvage, *J. Am. Chem. Soc.* **1992**, *114*, 4632–4639; b) H. L. Anderson, *Inorg. Chem.* **1994**, *33*, 972–981; c) S. Anderson, H. L. Anderson, A. Bashall, M. McPartlin, J. K. M. Sanders, *Angew. Chem.* **1995**, *107*, 1196-1200; *Angew. Chem. Int. Ed. Engl.* **1995**, *34*, 1096–1099; d) P. N. Taylor, H. L. Anderson, *J. Am. Chem. Soc.* **1999**, *121*, 11538–11545; e) C. C. Mak, N. Bampos, J. K. M. Sanders, *Angew. Chem.* **1998**, *110*, 3169–3172; *Angew. Chem. Int. Ed.* **1998**, *37*, 3020–3023; f) C. A. Hunter, R. K. Hyde, *Angew. Chem.* **1996**, *108*, 2064–2067; *Angew. Chem. Int. Ed. Engl.* **1996**, *35*, 1936–1939; g) S. Rucareanu, O. Mongin, A. Schuwey, N. Hoyler, A. Gossauer, *J. Org. Chem.* **2001**, *66*, 4973–4988; h) C. M. Drain, F. Nifiatis, A. Vasenko, J. D. Batteas, *Angew. Chem.* **1998**, *110*, 2478–2481; *Angew. Chem. Int. Ed.* **1998**, *37*, 2344–2347; i) K. Ogawa, Y. Kobuke, *Angew. Chem.* **2000**, *112*, 4236–4239; *Angew. Chem. Int. Ed.* **2000**, *39*, 4070–4073; j) H. A. M. Biemans, A. E. Rowan, A. Verhoeven, P. Vanoppen, L. Latterini, J. Foekema, A. P. H. J. Schenning, E. W. Meijer, F. C. de Schryver, R. J. M. Nolte, *J. Am. Chem. Soc.* **1998**, *120*, 11054–11060; k) J. L. Sessler, B. Wang, A. Harriman, *J. Am. Chem. Soc.* **1995**, *117*, 704–714; l) C. M. Drain, K. C. Russel, J.-M. Lehn, *Chem. Commun.* **1996**, 337–338; m) C. Ikeda, N. Nagahara, E. Motegi, N. Yoshioka, H. Inoue, *Chem. Commun.* **1997**, 1759–1760; n) Y. Kuroda, K. Sugou, K. Sasaki, *J. Am. Chem. Soc.* **2000**, *122*, 7833–7834; o) K. Sugou, K. Kitajima, T. Iwaki, Y. Kuroda, *J. Am. Chem. Soc.* **2002**, *124*, 1182–1183.

[3] a) J. H. Fendler, *Membrane Mimetic Chemistry*, Wiley, New York, **1982**; b) S. Baral, J. H. Fendler in *Photoinduced Electron Transfer*, *Part B*, *Experimental Techniques and Medium Effects* (Eds.: M. A. Fox, M. Chanon), Elsevier, Amsterdam, **1988**, pp. 541–598; b) J.-H. Fuhrhop, J. Köning, *Membranes and Molecular Assemblies: The Synkinetic Approach*, The Royal Society of Chemistry, Cambridge, **1994**.

[4] a) T. J. Dannhauser, M. Nango, N. Oku, K. Anzai, P. A. Loach, *J. Am. Chem. Soc.* **1986**, *108*, 5865–5871; b) M. Nango, K. Iida, M. Yamaguchi, Y. Yamashita, K. Tsuda, A. Mizusawa, T. Miyake, A. Masuda, J. Yoshinaga, *Langmuir* **1996**, *12*, 1981–1988; c) J. Lahiri, G. D. Fate, S. B. Ungashe, J. T. Groves, *J. Am. Chem. Soc.* **1996**, *118*, 2347–2358.

[5] a) M. Calvin, *Acc. Chem. Res.* **1978**, *11*, 369–374; b) T. Matsuo, K. Itoh, K. Takaku, K. Hashimoto, T. Nagamura, *Chem. Lett.* **1980**, 1009–1012; c) J. K. Hurst, L. Y. C. Lee, M. Grätzel, *J. Am. Chem. Soc.* **1983**, *105*, 7048–7056; d) E. Tsuchida, M. Kaneko, H. Nishide, H. Hoshino, *J. Phys. Chem.* **1986**, *90*, 2283–2284; e) G. Steinberg-Yfrach, P. A. Liddell, S.-C. Hung, A. L. Moore, D. Gust, T. A. Moore, *Nature* **1997**, *385*, 239–241.

[6] a) K. Eshima, M. Yuasa, H. Nishide, E. Tsuchida, *J. Chem. Soc. Chem. Commun.* **1985**, 130–132; b) E. Tsuchida, H. Nishide, *Top. Curr. Chem.* **1986**, *132*, 64–99; c) E. Tsuchida, H. Nishide, M. Yuasa, E. Hasegawa, K. Eshima, Y. Matsushita, *Macromolecules* **1989**, *22*, 2103–2107.

[7] a) J. T. Groves, R. Neumann, *J. Am. Chem. Soc.* **1989**, *111*, 2900–2909; b) A. P. H. J. Schenning, J. H. L. Spelberg, M. C. P. F. Driessen, M. J. B. Hauser, M. C. Feiters, R. J. M. Nolte, *J. Am. Chem. Soc.* **1995**, *117*, 12655–12656; c) Y. Naruta, M. Goto, T. Tawara, F. Tani, *Chem. Lett.* **2002**, 162–163.

[8] G. Steinberg-Yfrach, J.-L. Rigaud, E. N. Durantini, A. L. Moore, D. Gust, T. A. Moore, *Nature* **1998**, *392*, 479–482.

[9] a) J.-H. Fuhrhop, U. Bindig, U. Siggel, *J. Am. Chem. Soc.* **1993**, *115*, 11036–11037; b) C. Endisch, C. Böttcher, J.-H. Fuhrhop, *J. Am. Chem. Soc.* **1995**, *117*, 8273–8274.

[10] J.-H. Fuhrhop in *Comprehensive Supramolecular Chemistry*, *Templating*, *Self-assembly*, *and Self-organization*, *Vol. 9* (Eds.: J.-M. Lehn, J. L. Atwood, J. E. D. Davies, D. D. MacNicol, F. Vögtle), Pergamon, Oxford, **1996**, pp. 407–450.

[11] a) R. Guilard, N. Senglet, Y. H. Liu, D. Sazou, E. Findsen, D. Fanre, T. D. Courieres, K. M. Kadish, *Inorg. Chem.* **1991**, *30*, 1898–1905; b) J.-H. Fuhrhop, C. Demoulin, C. Böttcher, J. Köning, U. Siggel, *J. Am. Chem. Soc.* **1992**, *114*, 4159–4165; c) T. Komatsu, K. Nakao, H. Nishide, E. Tsuchida, *J. Chem. Soc. Chem. Commun.* **1993**, 728–730; d) E. Tsuchida, T. Komatsu, N. Toyano, S. Kumamoto, H. Nishide, *J. Chem. Soc. Chem. Commun.* **1993**, 1731–1733; e) E. Tsuchida, T. Komatsu, K. Arai, K. Yamada, H. Nishide, C. Böttcher, J.-H. Fuhrhop, *J. Chem. Soc. Chem. Commun.* **1995**, 1063–1064; f) T. Komatsu, K. Yamada, E. Tsuchida, U. Siggel, C. Böttcher, J.-H. Fuhrhop, *Langmuir* **1996**, *12*, 6242–6249; g) T. Komatsu, E. Tsuchida, C. Böttcher, D. Donner, C. Messerschmidt, U. Siggel, W. Stocker, J. P. Rabe, J.-H. Fuhrhop, *J. Am. Chem. Soc.* **1997**, *119*, 11660–11665; h) T. Komatsu, T. Yanagimoto, E. Tsuchida, U. Siggel, J.-H. Fuhrhop, *J. Phys. Chem. B* **1998**, *102*, 6759–6765; i) T. Komatsu, T. Yanagimoto, Y. Furubayashi, J. Wu, E. Tsuchida, *Langmuir* **1999**, **15**, 4427–4433; j) S. Schell, H. K. Hombrecher, *Chem. Eur. J.* **1999**, *5*, 587–598; k) K. Kano, K. Fukuda, H. Wakami, R. Nishiyabu, R. F. Pasternack, *J. Am. Chem. Soc.* **2000**, *122*, 7494–7502; l) T. Komatsu, S. Hayakawa, T. Yanagimoto, M. Kobayakawa, A. Nakagawa E. Tsuchida, *Bull. Chem. Soc. Jpn.* **2001**, *74*, 1703–1707; m) N. Nagata, S. Kugimiya, Y. Kobuke, *Chem. Commun.* **2001**, 689–690.

[12] a) E. Tsuchida, T. Komatsu, K. Arai, H. Nishide, *J. Chem. Soc. Chem. Commun.* **1993**, 730–732; b) E. Tsuchida, T. Komatsu, K. Arai, K. Yamada, H. Nishide, C. Böttcher, J.-H. Fuhrhop, *Langmuir* **1995**, *11*, 1877–1884.

[13] Y. Matsushita, E. Hasegawa, K. Eshima, E. Tsuchida, *Chem. Lett.* **1983**, 1387–1390.

  0947-6539/02/0823-5479 $ 20.00+.50/0

[14] J. H. Espenson, R. J. Cristiensen, *Inorg. Chem.* **1977**, *16*, 2561 – 2564.
[15] G. Roberts, *Langmuir – Blodgett*, Plenum Press, New York, **1990**; b) K. Larsson in *The Lipid Handbook* (Eds.: F. D. Gunstone, J. L. Harwood, F. B. Padley), Chapman and Hall, London, **1986**, pp. 321 – 382.
[16] a) E. G. McRae, M. Kasha, *J. Chem. Phys.* **1958**, *28*, 721 – 722; b) M. Kasha, *Radiation Res.* **1963**, *20*, 51 – 71.
[17] a) M. P. Byrn, C. J. Curtis, I. Goldberg, Y. Hsiou, S. I. Khan, P. A. Sawin, S. K. Tendick, C. E. Strouse, *J. Am. Chem. Soc.* **1991**, *113*, 6549 – 6557; b) M. P. Byrn, C. J. Curtis, Y. Hsiou, S. I. Khan, P. A. Sawin, S. K. Tendick, A. Terzis, C. E. Strouse, *J. Am. Chem. Soc.* **1993**, *115*, 9480 – 9497.
[18] C. A. Hunter, J. K. M. Sanders, A. J. Stone, *Chem. Phys.* **1989**, *133*, 395 – 404.
[19] U. Siggel, C. Endisch, T. Komatsu, E. Tsuchida, J. Voigt, J.-H. Furhop, *Ber. Bunsen-Ges.* **1996**, *100*, 2070 – 2075.
[20] D. C. Barber, R. A. Freitag-Beeston, D. G. Whitten, *J. Phys. Chem.* **1991**, *95*, 4074 – 4086.
[21] C. Odin, J. P. Aimé, Z. El Kaakour, T. Bouhacina, *Surf. Sci.* **1994**, *317*, 321 – 340.
[22] a) J. P. Collman, R. R. Gagne, C. A. Reed, T. R. Halbert, G. Lang, W. T. Robinson, *J. Am. Chem. Soc.* **1975**, *97*, 1427 – 1439; b) J. R. Budge, P. E. Ellis, Jr., R. D. Jones, J. E. Linard, F. Basolo, J. E. Baldwin, R. L. Dyer, *J. Am. Chem. Soc.* **1979**, *101*, 4760 – 4762; c) M. Momenteau, B. Loock, E. Bisagni, M. Rougee, *Can. J. Chem.* **1979**, *57*, 1804 – 1813.
[23] H. F. Bunn, B. G. Forget, *Hemoglobin: Molecular, Genetic and Clinical Aspects*, W. B. Sunders Company, Philadelphia, **1986**.
[24] a) D. W. Deamer, A. D. Bangham, *Biochim. Biophys. Acta.* **1976**, *443*, 629 – 634; b) M. Pozansky, S. Tong, P. C. White, J. M. Milgram, A. K. Solomon, *J. Gen. Physiol.* **1976**, *67*, 46 – 66.
[25] a) J. P. Collman, J. I. Brauman, K. M. Doxsee, T. R. Halbert, E. Bunnenberg, R. E. Linder, G. N. LaMar, J. D. Guadio, G. Lang, K. Spartalian, *J. Am. Chem. Soc.* **1980**, *102*, 4182 – 4192; b) J. P. Collman, F. Basolo, E. Bunnenberg, T. C. Collins, J. H. Dawson, P. E. Ellis, M. L. Marrocco, A. Moscowitz, J. L. Sessler, T. Szymanski, *J. Am. Chem. Soc.* **1981**, *103*, 5636 – 5648; c) J. P. Collman, J. I. Brauman, T. J. Collins, B. L. Iverson, G. Lang, R. B. Pettman, J. L. Sessler, M. A. Walters, *J. Am. Chem. Soc.* **1983**, *105*, 3038 – 3052.
[26] a) J. P. Collman, J. I. Brauman, T. R. Halbert, K. S. Suslick, *Proc. Natl. Acad. Sci. USA* **1976**, *73*, 3333 – 3337; b) E. Tsuchida, T. Komatsu, T. Nakata, E. Hasegawa, H. Nishide, H. Inoue, *J. Chem. Soc. Dalton Trans.* **1991**, 3285 – 3289.
[27] a) C. H. Barlow, J. C. Maxwell, W. J. Wallace, W. S. Caughey, *Biochem. Biophys. Res. Commun.* **1973**, *55*, 91 – 95; b) W. S. Caughey, *Ann. N. Y. Acad. Sci.* **1970**, *174*, 148 – 153.
[28] T. Komatsu, S. Ishihara, H. Nishide, E. Tsuchida, unpublished results.
[29] R. H. Pearson, I. Pascher, *Nature* **1979**, *281*, 499 – 501.
[30] G. McDermott, S. M. Prince, A. A. Freer, A. M. Hawthornthwaite-Lawless, M. Z. Papiz, R. J. Cogdell, N. W. Isaacs, *Nature* **1995**, *374*, 517 – 521.

Received: May 22, 2002 [F4116]

  0947-6539/02/0823-5480 $ 20.00+.50/0